Available online at www.sciencedirect.com
SCIENCE DIRECT®
Journal of Nuclear Materials 337–339 (2005) 154–160
journal of nuclear materials
www.elsevier.com/locate/jnucmat

Local island divertor experiments on LHD

T. Morisaki [a,*], S. Masuzaki [a], A. Komori [a], N. Ohyabu [a], M. Kobayashi [a], Y. Feng [b], F. Sardei [b], K. Narihara [a], K. Tanaka [a], K. Ida [a], B.J. Peterson [a], M. Yoshinuma [a], N. Ashikawa [a], M. Emoto [a], H. Funaba [a], M. Goto [a], K. Ikeda [a], S. Inagaki [a], O. Kaneko [a], K. Kawahata [a], S. Kubo [a], J. Miyazawa [a], S. Morita [a], K. Nagaoka [a], Y. Nagayama [a], H. Nakanishi [a], K. Ohkubo [a], Y. Oka [a], M. Osakabe [a], T. Shimozuma [a], M. Shoji [a], Y. Takeiri [a], S. Sakakibara [a], R. Sakamoto [a], K. Sato [a], K. Toi [a], K. Tsumori [a], K.Y. Watababe [a], H. Yamada [a], I. Yamada [a], Y. Yoshimura [a], O. Motojima [a], LHD Experimental Group [a]

[a] *National Institute for Fusion Science, 322-6 Orosi, Toki, Gifu 509-5292, Japan*
[b] *Max-Planck-Institute für Plasmaphysik, Euratom Association Teilinstitut Greifswald, Wendelsteinstrasse 1, D-17491 Greifswald, Germany*

Abstract

A local island divertor (LID) experiment has begun on LHD, with the aims of controlling edge recycling and improving the plasma confinement. The fundamental divertor functions of the LID have been demonstrated in the recent experiments. From the particle flux profile measurements on the LID head it was found that the particles diffusing out from the core region are well guided along the island separatrix to the LID head. Owing to the closed configuration around the LID head, evidence of the high efficient pumping was observed, together with a strong capacity to screen impurities. The first results of edge modeling using the EMC3-EIRENE code are also presented.

PACS: 52.55.Hc
Keywords: LHD; Island divertor; Edge modeling; Edge plasma; Impurity screening

1. Introduction

In the large helical device (LHD) project [1], divertor research is one of the most important goals in the mission to achieve high quality helical plasmas relevant to a fusion reactor. The divertor is expected to play a key role in improving the plasma performance through edge control.

In LHD, two completely different divertor magnetic geometries are employed, i.e., the helical divertor (HD) and the local island divertor (LID). The HD is similar to the tokamak double null divertor except for the long connection length of the field lines in the

* Corresponding author. Tel.: +81 572 58 2146; fax: +81 572 58 2618.
E-mail address: morisaki@nifs.ac.jp (T. Morisaki).

0022-3115/$ - see front matter © 2004 Elsevier B.V. All rights reserved.
doi:10.1016/j.jnucmat.2004.10.165

thick ergodic region surrounding the closed surfaces [2]. The LID is an alternative, innovative concept [3] utilized for edge plasma control, prior to the full-scale HD operation. The advantage of LID over HD is the technical ease of pumping in the closed system, since recycling is toroidally and poloidally localized in a small region. This may contribute to great reduction of the construction cost, compared to the full closed HD system.

After numerical studies and preliminary experiments on the compact helical system (CHS), the LID experiment on LHD has been in operation since 2002 [4,5]. Overcoming some troubles in the first experimental phase, full-scale operation with heating power of more than 10 MW could be performed in the last experimental campaign.

In this paper experimental results mainly from the last experimental campaign are summarized after the brief description of the principle and hardware of LID. Remarkable progress in the modeling study which strongly supports the experimental research is also presented.

2. LID configuration and hardware

The LID is a kind of the island divertor [6] which utilizes a superimposed $m/n = 1/1$ island located in the edge region, where m and n are poloidal and toroidal mode numbers, respectively. By inserting the LID head into the island from the outboard side of the torus, field lines of the island are cut by the LID head and its supporting rod, thus removing all closed flux surfaces around the edge region.

Particles diffusing out from the core region cross the island separatrix and flow along the periphery of the island. After several toroidal turns, they reach the outer separatrix of the island where the LID head is placed, and strike its backside on which they are neutralized, as shown in Fig. 1. Since the LID head is inserted deeply in the island, the leading edge of the head is safe from high heat flux. The position of the LID head, r_{head}, is defined as the horizontal distance from the outer island separatrix to its leading edge, as depicted in Fig. 1. In other words, r_{head} is the depth of the leading edge in the island, with a minus sign. Particles recycled there are pumped out efficiently by the strong pumping system with a baffle integrated into the closed divertor configuration. Note that LID is not a pumping limiter but a genuine divertor, because the LID head never scrapes off plasma from the confinement region. In the LID configuration, the boundary of the confinement region is defined with the inner island separatrix.

The LID system consists of two parts, i.e., the perturbation coils and the LID head system. For generating an

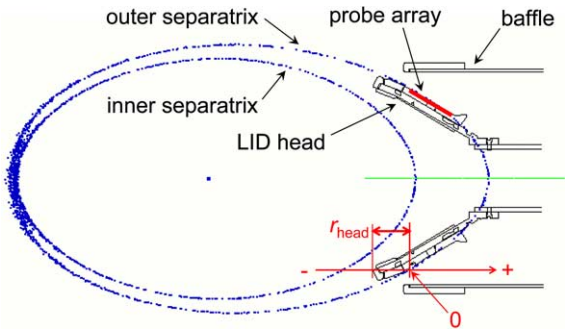

Fig. 1. A schematic of the LID. The LID head position, r_{head}, is defined as the horizontal distance from the outer island separatrix to its leading edge.

$m/n = 1/1$ island, 10 pairs of small normal conducting loop coils are installed at the top and bottom of the torus. Three power supplies drive these coils, and can generate a 0.23 m wide island at the position where the LID head is located. The LID head system consists mainly of a divertor head surrounded with a baffle, vacuum pumps and a translation mechanism. The LID head whose size is about $1\,m \times 0.6\,m \times 0.4\,m$ has a highly complicated three dimensional (3D) shape to fit into the island structure. Great efforts were paid to the design of the geometrical shape of the LID head in order to withstand heat fluxes of $\sim$7.5 MW/m^2 for 5 s, that is, angles between tiles and magnetic field lines are kept less than 10° everywhere on it. The surface of the LID head is covered with carbon and partially with molybdenum tiles to withstand the high heat loads. The tiles are mechanically joined to a stainless steel heat sink on which water cooling channels are grooved. Thin carbon sheets are sandwiched between the tiles and the heat sink to increase the contact area. Since the divertor head itself is electrically isolated from the vacuum vessel and supporting structure, a bias voltage up to 1 kV can be applied. The divertor head is surrounded by a baffle to realize a closed divertor system. The LID head and the baffle can move independently in the radial direction by separate translation mechanisms, hence the width of the slit between them can be changed to maximize the pumping efficiency. Some diagnostics are built into the LID head system. For flux measurements 39 Langmuir probes and 22 thermocouples are embedded in the carbon tiles. Image guide fibers for two dimensional profile measurements and a bundle fiber for visible spectroscopy are also installed inside the baffle, viewing the divertor head from its backside. In order to estimate the pumping efficiency, an ASDEX style gauge is installed inside the baffle. By using the eight cryogenic pumps, an effective hydrogen pumping speed of 111 m^3/s at the gate valve between LHD and the LID chamber is achieved.

3. Experimental setup

The LHD is the largest superconducting heliotron device with poloidal/toroidal period numbers of 2/10, major and averaged plasma minor radius of 3.6–4.0 m and 0.6 m, respectively. Three neutral beams (NB) with the total heating power up to ~10 MW are injected to generate and heat the LHD plasma. For fueling, LHD is equipped with four gas puff valves and two frozen H_2 pellet injectors. The LID head is inserted into the plasma from the outboard side of the torus where the O-point of the $m/n = 1/1$ island is located. At this poloidal cross-section, the plasma is horizontally elongated and the island width is at the maximum (refer to Fig. 1). Major diagnostics in LHD are utilized to measure plasma parameters. Thomson scattering system provides the electron temperature T_e profile and a rough measure of the electron density. The line averaged density is measured with the far infrared interferometer (FIR). Radiation from impurities are measured with the bolometer array and impurity densities with the charge exchange recombination spectroscopy system (CXRS). The visible and VUV spectroscopy systems are also employed to diagnose impurity ions and recycling particles. Plasma stored energy is measured with diamagnetic loop.

4. Results

4.1. Basic function of LID and typical discharge

Typical T_e profiles of LID (closed red circles) and HD (open red) discharges, together with the Poincare plot of the island separatrix at Thomson scattering system are presented in Fig. 2. The intensity profile, I_{TS}, of the scattered light (blue) is also shown as an index of the electron density. Note that the phase of the island at Thomson scattering location is different from that at the toroidal position where the LID head is inserted, since they are 72° apart from each other in the toroidal direction. It is clearly seen that T_e rises from the inner separatrix of the island. The I_{TS} profile is broader than the T_e profile. Namely, I_{TS} rises from the outer separatrix of the island and changes its gradient at the inner separatrix of the island. Relatively high dense but low temperature plasma remains in the island region. The I_{TS} profile is hollow in the island core, as shown in Fig. 2. The explanation is that field lines connecting the boundary of the confinement region to the LID head along the island separatrix are long enough to confine such low temperature plasmas, while the parallel transport is still dominant for energy flow. An interesting feature also observed in the T_e and I_{TS} profiles is that small peaks exist at the outer separatrix of the island. It is evident that the island separatrix indeed guides heat and particle fluxes to the LID head. Furthermore the very steep gradient formed in the T_e profile of the LID discharge is remarkable, which is due to the local confinement improvement in the edge region compared with the HD discharge.

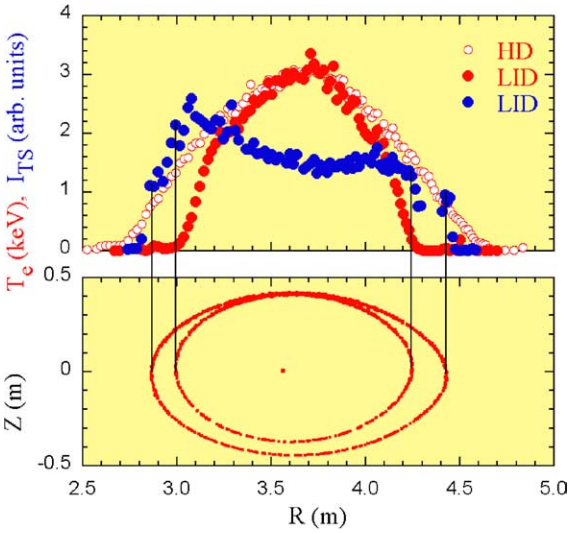

Fig. 2. Typical T_e profiles of LID (closed red circles) and HD (open red) discharges, together with a Poincare plot of the island separatrix at Thomson scattering system. The intensity profile, I_{ts}, of the scattered light (blue) is also depicted as measure of the electron density.

In order to optimize the LID configuration, the LID head position was scanned under the same experimental conditions, i.e., with the same NB power and the same gas puffing rate. Fig. 3 shows the line averaged electron density $\bar{n}_e$, plasma stored energy normalized by the averaged density $W_{dia}/\bar{n}_e$ and density decay time τ_p^*, at the various LID head positions, where τ_p^* is a characteristic time for the density decay after turning off the gas puff. Employing the recycling coefficient R, τ_p^* can be described as $\tau_p^* = \tau_p/(1-R)$ where τ_p is the particle confinement time. It is clearly shown that $\bar{n}_e$ and τ_p^* are at the minimum and $W_{dia}/\bar{n}_e$ reaches the maximum at $r_{head} \sim -100$ mm. This is where the leading edge of the LID head is completely in the island but it never touches the inner separatrix of the island. At this position, the LID operates at its best, i.e., with maximum pumping efficiency and consequently maximum $W_{dia}/\bar{n}_e$. Another experimental result also supports this assertion. Fig. 4 represents the T_e profiles for three different LID head positions. It is found that the highest temperature is achieved when the LID head is at its optimum position of $r_{head} = -108$ mm. This figure also shows other important information. For these three different profiles, although the LID head changes its position by 60 mm, the edge of the T_e profile, where it rises, changes little. In short, over the range $-108\ \text{mm} < r_{head} < -48$ mm, the LID head is in the island. Under this optimized configuration

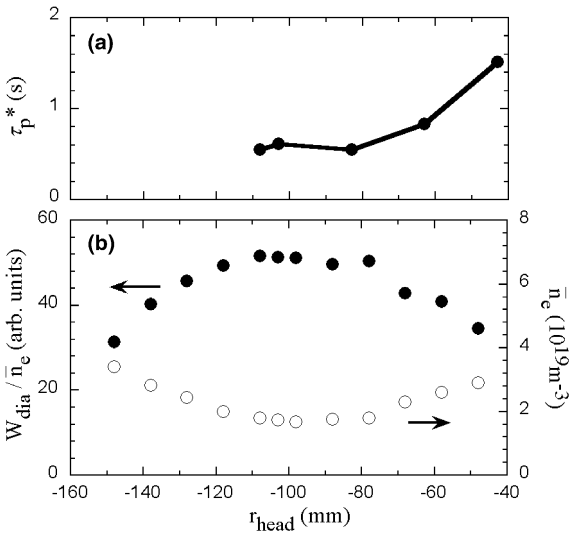

Fig. 3. The LID head position r_{head} dependence on (a) effective confinement time, τ_p^*, (b) stored energy normalized by line averaged density, $W_{dia}/\bar{n}_e$, and line averaged density, $\bar{n}_e$.

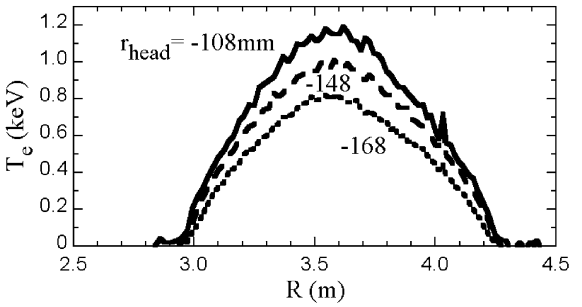

Fig. 4. The electron temperature, T_e, profiles for different LID head positions.

with $r_{head} \sim -100$ mm, following experiments and numerical simulations were carried out.

In Fig. 5, the particle flux (ion saturation current) profile on the LID head measured with the Langmuir probe array is shown. Probes with smaller numbers are located nearest the leading edge of the LID head. The distance between adjacent probes is about 10 mm in real space (on tiles) but the projected distance onto flux surfaces in the radial direction is reduced to less than a few millimeter, since the angle between the field line and the tile is shallow. In Fig. 5, the leading edge is located about several centimeter left from probe # 1. It can be seen that the particle flux near the leading edge is small, then gradually increases with distance from the leading edge, and has its maximum around probes # 6–8. After that, the particle flux decreases monotonically. From this experimental result and the numerical calculation of the magnetic field structure, it is confirmed that the peak in the flux profile corresponds to the outer separatrix of the island. In summary, the particle flux surely flows to the LID head along the outer separatrix of the island, making its way around the leading edge, which is the ideal situation expected in the physical design concept. However, we cannot conclude that the LID is completely free from a leading edge problem. Although most of the leading edge is safe from high heat loads, to be sure, at the small part of the leading edge, a few hot spots are observed in the camera images. These hot spots are located on some misaligned tiles jutting out from the rest. These hot spots are connected to each other with relatively short magnetic field lines. In order to solve this problem, the LID head should be shaped perfectly to fit the magnetic flux surface of the island. However it is quite difficult to shape the LID head so precisely. Thus, in reality, the best design is, as much as possible, to keep the distance from the inner island separatrix to the leading edge long.

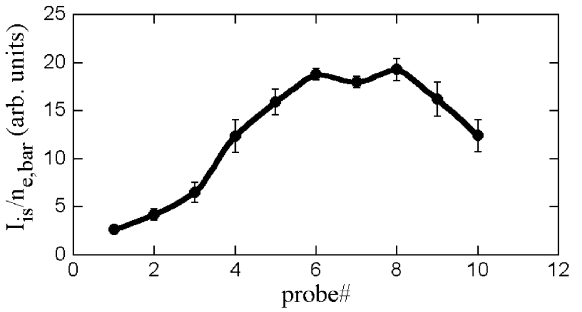

Fig. 5. The ion saturation current profile on LID head.

4.2. Modeling study

The inherent three dimensionality of the magnetic field structure in LHD always brings severe difficulties in modeling the edge transport with any simplified 1D or 2D treatments. Recently, the edge transport physics has been analyzed using the 3D fluid edge transport code, EMC3 [7], coupled with the kinetic neutral transport code, EIRENE [8]. With the advantage of the Monte Carlo scheme, the code can treat almost any arbitrary three dimensional geometry of plasma, magnetic field and plasma facing components, and provide 3D profiles of plasma parameters, i.e., n_e, T_e, T_i, $V_{\parallel}$, neutrals, etc.

In the modeling discussed here, the EMC3-EIRENE code simulated a discharge with relatively low heating power, i.e., $P_{NB} \sim 1.4$ MW using the vacuum magnetic field configuration calculated with the field line tracing code KMAG [9]. Although the plasma has finite pressure in the LID experiment, the measured beta value is small enough to be neglected its effect. The electron density at the inner island separatrix was set at

$n_e \sim 1.2 \times 10^{19}\ m^{-3}$ referring to the experimental measurement to be simulated. The LID head position of $r_{head} = -118$ mm for the reference shot was also set in the code. In Fig. 6, some results of the EMC3-EIRENE prediction are shown, i.e., two dimensional profiles of (a) electron density described as the logarithmic scale normalized by the maximum value of $2.5 \times 10^{20}\ m^{-3}$, (b) electron temperature, (c) particle flux, and (d) neutralized hydrogen molecule density, on a poloidal cut at the LID head. The cross-section of the LID head is outlined as a white background (refer to Fig. 1). The baffle surrounding the LID head and the island separatrix are also depicted in the figure. From Fig. 6(a) and (c), it can be seen that parallel flow is established along the separatrix toward the LID head, and that the highest density is achieved at the strike point of the outer separatrix on the LID head, which agrees well with the experimental result depicted in Fig. 5. The explanation is that particles diffusing out from the confinement region are well guided to the LID head along the island separatrix.

The flow profile in Fig. 6(c) shows a small amount of particle flow onto the front side of the LID head and the leading edge. This is also observed in the experiment, as described in Section 4.1. This unfavorable deposition consequently enhances the local recycling, which can be seen in the neutral profile, as shown in Fig. 6(d). From the simulations, 20% of the total particle flux was found to be deposited on the front side and the leading edge. This situation degrades the pumping efficiency, since neutralized particles in the unfavorable region

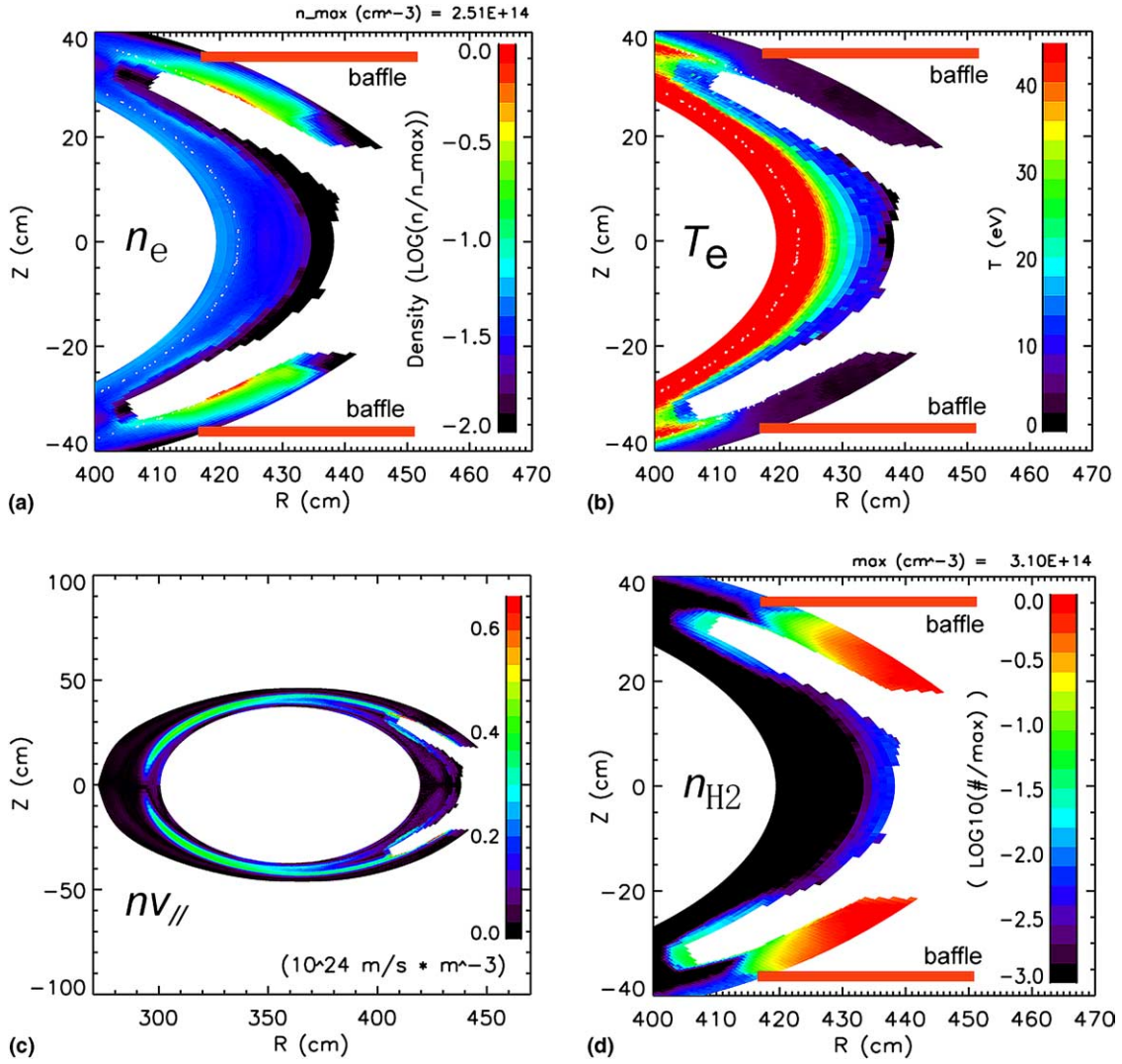

Fig. 6. 2D profiles of (a) electron density, n_e, (b) electron temperature, T_e, (c) flow, $v_{\parallel}$, and (d) hydrogen molecule density, n_{H2}, near the LID head, predicted by the EMC3-EIRENE code.

cannot be trapped by the baffle. The pumping efficiency would be a key factor in realizing the best divertor performance, for which the head design has to be optimized taking into account the edge transport process. With the present LID head, the EMC3-EIRENE code estimates a pumping efficiency, ε, at 50–60% under the definition of $\varepsilon = \Gamma_{\text{pump}}/\Gamma_{\text{head}}$, where Γ_{pump} and Γ_{head} are the particle flux pumped out by LID and the particle flux coming to the LID head, respectively. Particle flux recycled at the LID head is excluded from the definition of Γ_{head}, which accounts for more than 90% of whole recycling.

As shown in Fig. 6(d), the closed structure of the divertor with the baffle gives rise to the high confinement performance for neutrals, up to $3.1 \times 10^{20}\ \text{m}^{-3}$. This leads to strong particle recycling, resulting in $T_e \sim 5$ eV, $n_e \sim 10^{19}$–$10^{20}\ \text{m}^{-3}$ just above the LID head surface, as shown in Fig. 6(a) and (b). The ion saturation current expected with these T_e and n_e roughly agrees to that measured with embedded probes in the experiment. In this parameter range, the ionization mean free path for neutrals is about several centimeter, which is comparable to the plasma thickness around the LID head.

In the experiment, an indication of the divertor detachment has been observed in the ion saturation current measured with the embedded probes in the LID head under particular experimental conditions. However, the EMC3-EIRENE code does not show the evidence of the divertor detachment. In the present computations, impurity transport was switched off. This is probably the reason why the temperature is still too high to have a substantial amount of volume recombination process leading to detachment. Exploring the detachment regime is a next step of the modeling study.

4.3. Impurity control

It has been found that the LID is capable of pumping out the plasmas in the edge region and controlling them. Based on these experimental and modeling results, the function of the LID for impurity control is investigated. First of all, radiation profiles as a function of the normalized radius, ρ, were measured with the bolometer array, comparing the LID configuration to the HD configuration, as shown in Fig. 7. Blue and red lines are for the HD and LID configurations, respectively. A distinct difference between the two configurations is the radiation power itself, which is about 50% lower for LID over HD configurations over the entire plasma, except for the plasma center in relatively high density operations. It can also be seen that the highly radiated region is different for each configuration. In the HD configuration the radiation is high in the region where $\rho > 0.65$. On the other hand, in the LID configuration, it is localized in the narrow edge region where the island is located (depicted with thick bar in Fig. 7). The cold and dense plasma in the island may play an important

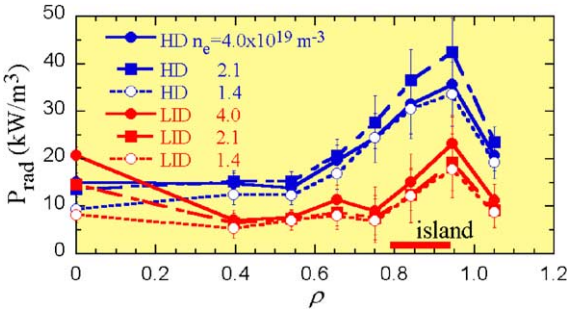

Fig. 7. Radial radiation profiles for HD (blue) and LID (red) configurations, as a function of normalized radius ρ.

role in the radiation process. As mentioned before, the radiation from the central region increases as the averaged density in the LID configuration, which finally exceeds that found for HD operation for densities of over $2.1 \times 10^{19}\ \text{m}^{-3}$. The main sources of the radiation are metallic impurities which may be released from the LID head heated up by the high heat and particle flux. There is a possibility that this high radiation from the central region may degrade the core plasma performance if the impurity accumulates further. It is necessary to make an effort to reduce impurities from the hot spots on the LID head as much as possible.

In order to investigate the impurity shielding effect of the LID, neon (Ne) was injected to the hydrogen plasma by gas puffing with a gas inlet 126° apart from the LID head in the toroidal direction. In this geometry, most of Ne is ionized near the *X*-point of the island. Fig. 8 shows the Ne density profiles measured with the CXRS for the HD and LID configurations. The zone where the island exists is indicated with the thick bar on the abscissa in the figure. The island width is small (a few centimeter) as depicted in the figure, because CXRS is measured near the *X*-point of the island. The Ne densities in Fig. 8 are normalized by the Ne puffing rate, since the Ne gas puffing rate in the LID configuration is higher

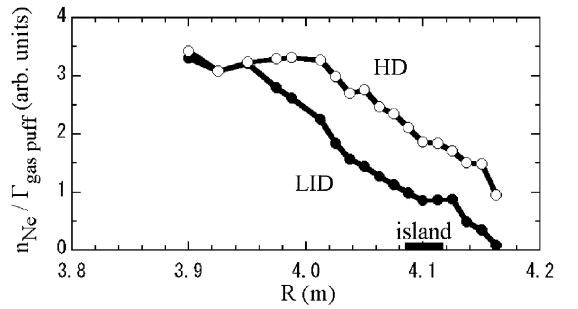

Fig. 8. Radial profiles of Ne density for HD (open circles) and LID (closed circles) configurations, normalized by Ne gas puffing rate.

than that in the HD configuration. From the figure, it is obvious that the Ne density in the LID configuration is lower than that in the HD configuration. Most of the injected Ne is shielded by the island and soon pumped out via the LID head. It is found that the LID is very effective for impurity screening.

5. Discussion

To see the confinement performance of the LID, the energy confinement time τ_E experimentally measured with the diamagnetic loop was compared with that derived from the ISS95 scaling law [10]. In general, it follows the ISS95 scaling law and unfortunately no obvious confinement improvement from the HD configuration has been seen. The database used here was accumulated in the inward shifted configuration with the magnetic axis position R_{ax} of 3.60 m where the best confinement performance has been achieved with the HD [11]. Searching for a breakthrough to the current situation, a preliminary trial in the outward shifted configuration of $R_{ax} = 3.75$ m was carried out at the final stage of the last experimental campaign, although the LID head shape is not optimized to the $R_{ax} = 3.75$ m configuration but designed to fit $R_{ax} = 3.60$ m. The result of this trial is surprising that the achieved density is largely extended to $\sim 1 \times 10^{20}$ m^{-3} with the pellet injection, and the stored energy exceeds 700 kJ, both of which are nearly two times higher than that obtained in the $R_{ax} = 3.60$ m configuration. Improvement is also seen in the gas puff shots. Employing the ISS95 scaling law confinement improvement is clear in the LID configuration in $R_{ax} = 3.75$ m, i.e., τ_E of some discharges is more than 1.2 times longer than that from ISS95, while τ_E in the HD configuration approximately follows the ISS95 scaling law.

One of the reason for the improvement in the $R_{ax} = 3.75$ m configuration is considered to relate to the edge magnetic field structure. In the $R_{ax} = 3.75$ m configuration, the width of the ergodic layer is larger than that in the $R_{ax} = 3.60$ m, thus the island separatrix in $R_{ax} = 3.75$ m is already in the ergodic sea. The edge magnetic field structure is slightly changed from the perfect LID configuration. Some field lines escape to the HD target plates through the HD separatrix before striking the LID head because of its radial excursion due to the high ergodic effect. In this situation, a certain amount of particle recycling occurs on the HD target plates where no closed system, e.g., baffles and/or pump for neutrals, is equipped. In fact, a longer density decay time, τ_p^*, and a higher Hα light emission at the plasma edge, suggesting higher particle recycling, are observed in the $R_{ax} = 3.75$ m configuration. These recycled particles contribute to the increase in density, which is usually much larger than those obtained by gas puffing. The LID head which is not optimized to the $R_{ax} = 3.75$ m island may also cause the enhanced recycling, since the ratio of the particles striking the leading edge of the LID head increases. Such a high recycling situation may be able to increase fueling, thus achieve the high density and stored energy in the outward shifted configuration.

6. Summary

Basic functions of LID were experimentally confirmed on LHD. The edge plasma can successfully be controlled by LID with its strong pumping effect, as expected. The availability of LID for impurity control was also verified through an impurity injection experiment. A newly discovered outward shifted configuration was found to be promising. It is important to study the confinement properties of this configuration, in order to search and reach for a better confinement regime.

It was also found that the EMC3-EIRENE code, newly applied for LHD, can simulate the LID experiment and provide the reasonable predictions. To benchmark this numerical prediction, further experimental verification is necessarily expected.

Acknowledgments

The authors would like to thank all members of device engineering group for their support and operation of the machine. This research is partially supported by the Grant-Aid for Scientific Research from MEXT of the Japanese government.

References

[1] O. Motojima et al., Phys. Plasmas 6 (1999) 7843.
[2] N. Ohyabu et al., Nucl. Fus. 34 (1994) 387.
[3] N. Ohyabu et al., J. Nucl. Mater. 145–147 (1987) 844.
[4] A. Komori et al., J. Nucl. Mater. 241–243 (1997) 967.
[5] T. Morisaki et al., Fus. Eng. Des. 65 (2003) 475.
[6] K. McCormick et al., J. Nucl. Mater. 313–316 (2003) 1131.
[7] Y. Feng et al., Plasma Phys. Control. Fus. 44 (2002) 611.
[8] D. Reiter, Juelich Report (1984) 1947.
[9] Y. Nakamura et al., J. Plasma Fus. Res. 69 (1993) 41.
[10] U. Stroth et al., Nucl. Fus. 36 (1996) 1063.
[11] H. Yamada et al., Plasma Phys. Control. Fus. 43 (2001) A55.